Oscilloscope measurement of the synchronous phase shift in an electron storage ring

R. H. A. Farias, Liu Lin, A. R. D. Rodrigues, and P. F. Tavares
LNLS, Laboratório Nacional de Luz Síncrotron, Cx. Postal 6192, CEP 13083-970, Campinas, Brazil

A. Hofmann
CERN-SL Division, Geneva, Switzerland
(Received 5 March 2001; published 12 July 2001)

We present a new technique to measure the synchronous phase shift in an electron storage ring. A digital sampling oscilloscope is used to observe the cavity and beam signals simultaneously, and the amplitude and relative phase are obtained from a Fourier transform of the time-domain data. This procedure gives 6 mdeg resolution and is largely insensitive to input signal amplitude variations. The measurement system was used to study the dependence of the synchronous phase shift on beam current, gap voltage, and beam energy in the Brazilian Synchrotron Light Source electron storage ring.

DOI: 10.1103/PhysRevSTAB.4.072801 PACS numbers: 29.20.–c

I. INTRODUCTION

The measurement of the shift in the phase of the stored electron beam with respect to the cavity voltage (the synchronous phase shift [1]) is a well-known procedure to determine various important beam parameters in an electron storage ring. The variation of the synchronous phase shift as a function of gap voltage has been used to determine the energy loss to synchrotron radiation [2], and its variation as a function of beam current has been used in several machines [2–5] to determine parasitic mode losses. In most of these measurements, rf phase detection techniques are used and commercial vector voltmeters or network analyzers are often the instruments of choice. More recently, a novel method was proposed by Podobedov and Siemann [6] to mix the cavity and beam signals down to audio frequencies, thus allowing the use of a fully digitized lock-in amplifier for the phase detection. Their work demonstrated the possibility of measuring the very small phase shifts to be expected from the newer low impedance machines.

All of these measurements suffer from various difficulties, including electronic noise and various systematic errors (e.g., slow phase drifts due to cable temperature variations), that make accurate determinations of the phase shifts difficult.

One important source of uncertainty in phase measurements is the inherent dependence of the measured phase on the signal amplitude for rf phase detectors. The dependence of the measured phase on amplitude is a basic feature of most rf phase detectors based on mixing techniques, and a typical value of the phase measurement variation due to input signal amplitude variation for a commercial rf vector voltmeter is 50 mdeg/dB [4].

Another source of systematic error in the determination of the synchronous phase shift with an rf phase detector is the fact that the input signal to such detectors must be a pure sine wave; i.e., harmonic contamination must be kept minimum. Although this is fairly easy for the cavity signal [since the cavity itself is a rather narrow band object, a simple low-pass filter to eliminate the higher order mode (HOM) contributions is enough to prepare the signal], it is much more difficult for the beam signal, particularly when only a few buckets are filled in the machine. The most common solution is to provide bandpass filtering with a high Q filter (Q's of several hundreds up to a few thousands have been used). The difficulty now is that a high Q filter also produces a phase shift which is a fast varying function of its resonant frequency (determined by the filter temperature). For the case of the Brazilian Synchrotron Light Source (LNLS) machine, a filter of $Q = 736$ would be necessary to provide 20 dB attenuation at the first revolution harmonics around the rf harmonic. Such a filter (e.g., a copper coaxial cavity filter) would present 1.4 deg/K of phase sensitivity to filter temperature changes, so that in order to reach 10 mdeg phase accuracy its temperature would have to be kept constant to within 0.007 K.

In this paper, we report on the use of a digital sampling oscilloscope to measure the synchronous phase shift in the LNLS electron storage ring. The time-domain data from the digital scope is Fourier analyzed, and the changes in the beam-to-cavity phase are determined from the individual phases obtained from the beam and cavity signals. Electronic noise is reduced by averaging many readings of the scope, and harmonic contamination effects are kept under control by the digital filtering provided by the fast-Fourier transform (FFT) analysis, thus avoiding the use of high Q analog filters for the beam signal. This phase measurement technique reached 6 mdeg resolution and is quite insensitive to signal amplitude variations: test bench measurements have shown less than ± 10 mdeg phase variation over a 10 dB input signal range.

This paper is organized as follows. Section II shows the basic expressions that relate the synchronous phase shift to the energy loss of an electron beam including the losses to synchrotron radiation as well as to the resistive impedance.

Section III describes the experimental technique and data analysis procedures and presents test bench results of the phase measurement system characterization. Section IV describes the measurement setup in the LNLS storage ring and presents results of phase shift measurements as a function of rf gap voltage (for different beam energies) and beam current.

II. THEORY

The energy loss per revolution of an electron in a storage ring consists of a part U_s due to the emission of synchrotron radiation and a part U_{pm} due to the interaction of the beam with the resistive impedance of the vacuum chamber (the parasitic mode loss). This total energy loss must be compensated by the rf voltage seen by the beam at the synchronous phase ϕ_s:

$$U = U_s + U_{pm} = eV_0 \sin\phi_s , \tag{1}$$

where V_0 is the peak rf voltage. The loss to the impedance can be expressed in terms of the parasitic mode loss factor

$$k_{pm} = \frac{U_{pm}}{eT_0 I_0} . \tag{2}$$

Here, T_0 is the revolution time and I_0 is the total beam current. Thus, each of the two components of the energy loss can be obtained from measurements of the synchronous phase shift as a function of rf voltage and beam current.

A. Measurement of the energy loss due to synchrotron radiation

For a small beam current the parasitic mode loss is small and can be neglected. The energy loss U_s due to synchrotron radiation determines the synchronous phase ϕ_s

$$eV_0 \sin\phi_s = U_s . \tag{3}$$

In the experiment, we measure a phase ϕ_m which is related to the actual synchronous phase by an unknown phase ϕ_0 due to delays ($\phi_s = \phi_m + \phi_0$), giving

$$\begin{aligned} eV_0 \sin\phi_m \cos\phi_0 + eV_0 \cos\phi_m \sin\phi_0 \\ = y \cos\phi_0 + x \sin\phi_0 = U_s . \end{aligned} \tag{4}$$

From a series of ϕ_m measurements versus rf voltage we get values for $x = eV_0 \cos\phi_m$ and $y = eV_0 \sin\phi_m$ to be used in a linear fit which determines the slope A and offset B in the relation

$$y = Ax + B = -x \tan\phi_0 + \frac{U_s}{\cos\phi_0} . \tag{5}$$

The energy loss U_s is given by

$$U_s = \frac{B}{\sqrt{1 + A^2}} . \tag{6}$$

B. Parasitic mode loss measurement

If the rf gap voltage is kept fixed and the current is varied (e.g., by means of a beam scraper), only the parasitic losses vary. Differentiating Eq. (1) with respect to the beam current, we obtain in linear approximation

$$\frac{dU_{pm}}{dI_0} = eV_0 \cos\phi_s \frac{d\phi_s}{dI_0} \tag{7}$$

or, in terms of the parasitic mode loss factor,

$$k_{pm} = \frac{V_0}{T_0} \cos\phi_s \frac{d\phi_s}{dI_0} . \tag{8}$$

Assuming that the parasitic losses are small so that the synchronous phase shift due to the current is also small, we can use the calculated absolute synchronous phase at vanishing current to obtain the loss factor from the slope of the synchronous phase shift as a function of current.

1. Bunch filling form factor

Most often, loss factor measurements are done with a single bunch, but in the LNLS machine at present no provision exists for single bunch operation and all experiments reported here were carried out either with a bunch train followed by a gap or with all bunches filled. In order to compare results from experiments with different filling patterns, we introduce the normalized loss factor K_{pm}, which is related to the directly measured loss factor k_{pm} through a filling form factor Γ

$$K_{pm} = \frac{hk_{pm}}{\Gamma} , \tag{9}$$

where h is the harmonic number. To calculate Γ, we consider a multibunch beam with a sequence of n adjacent bunches of equal intensity spaced by the revolution frequency with total current I_0 and total charge q. Each bunch has a Gaussian longitudinal distribution of rms width σ_t. The current of this bunch train is given by

$$I_n(t) = I_0 + \sum_{p=1}^{\infty} \sum_{k=1}^{n} I_p \cos[p\omega_0 (t + kT_0/h)] , \tag{10}$$

where

$$I_p = \frac{2I_0}{n} \exp(-p^2 \omega_0^2 \sigma_t^2/2) , \tag{11}$$

which can be expressed as

$$\begin{aligned} I_n(t) = I_0 + \sum_{p=1}^{\infty} I_p \{ \cos(p\omega_0 t) \cos[(n+1)x/2] \\ - \sin(p\omega_0 t) \sin[(n+1)x/2] \} \\ \times \frac{\sin(nx/2)}{\sin(x/2)} , \end{aligned} \tag{12}$$

with $x = \frac{k2\pi}{h}$. The beam power spectrum at harmonic $p\omega_0$ is therefore proportional to

$$\langle I_{np}^2\rangle = \frac{I_p^2}{2}\,\frac{\sin^2(np\pi/h)}{\sin^2(p\pi/h)} = \frac{2I_0^2}{n^2}\,\frac{\sin^2(np\pi/h)}{\sin^2(p\pi/h)}\,, \quad (13)$$

where we have neglected, for the moment, the dependence of I_p on frequency; i.e., we assume the bunch length to be short and take $I_p \approx 2I_0/n$. This assumption will be removed in the next subsection.

The component at the rf frequency (and its multiples $p = mh$) is

$$\langle I_{nh}^2\rangle = \frac{n^2 I_h^2}{2} = 2I_0^2\,, \quad (14)$$

which is independent of the number of bunches for a given total current.

If only one bunch is filled ($n = 1$) we have lines at each revolution frequency $p\omega_0$ which are all of equal amplitude within our approximation $\langle I_{1p}^2\rangle = \frac{I_p^2}{2} = 2I_0^2$. It is interesting to calculate the sum of the powers within the h revolution harmonics

$$\sum_{p=1}^{h}\langle I_{1p}^2\rangle = hI_p^2/2 = 2hI_0^2\,. \quad (15)$$

If all buckets are filled with equal current, $n = h$ and $I_{hp} = 0$ for all p except $p = mh$ and the power within the h revolution harmonics is

$$\sum_{p=1}^{h}\langle I_{hp}^2\rangle = \frac{I_p^2}{2} = 2I_0^2\,. \quad (16)$$

For these bunch trains, the lines contributing to the power spectrum are concentrated around the rf frequency and its harmonics. Therefore, measurements of the parasitic mode loss factor using bunch trains will probe the impedance mainly around harmonics of the rf frequency. Some resonances of narrow or medium bandwidth might be missed in the process. Accepting this limitation we continue by taking an average of the power spectrum within one rf frequency,

$$\frac{d\langle I_{np}^2\rangle}{d\omega} = \frac{\sum_{p=1}^{h}\langle I_{np}^2\rangle}{h\omega_0}\,. \quad (17)$$

The spectral power density of the general case normalized to that of the single bunch case gives the filling form factor:

$$\frac{k_{pm}}{K_{pm}} = \frac{\Gamma}{h} = \frac{d\langle I_{np}^2\rangle/d\omega(n\text{ bunches})}{d\langle I_{1p}^2\rangle/d\omega(1\text{ bunch})} = \frac{\sum_{p=1}^{h}\langle I_{np}^2\rangle}{2hI_0^2}\,. \quad (18)$$

This equation shows how the filling form factor can be measured directly from an observation of the amplitude of beam harmonics observed on a spectrum analyzer connected to a longitudinal beam pickup.

For a uniform fill $\Gamma = 1$, whereas for a single bunch $\Gamma = h$. Therefore, the loss for a uniform fill is h times smaller than for a single bunch of the same total current, which makes the measurement more difficult.

2. Bunch length dependence and the impedance model

So far we have treated the line spectrum of the bunch pattern only up to the rf frequency and have neglected the effect of the finite bunch length. This was justified since the bunch is much shorter than the rf wavelength. To extend the bunch power spectrum to higher frequencies including the effect of the bunch length we have

$$\frac{d\langle I^2\rangle}{d\omega} \approx e^{-\omega^2/\sigma_\omega^2}\,\frac{\sum_{p=1}^{h}\langle I_{np}^2\rangle}{h\omega_0} = \frac{2I_0^2\Gamma}{h\omega_0}\,e^{-\omega^2\sigma_t^2}, \quad (19)$$

where $\sigma_\omega = 1/\sigma_t$. To calculate the energy loss of the beam we take a model for the impedance in the form of a broad band resonator with $Q = 1$, a resonant frequency ω_r, and a shunt impedance $R_s = |Z/n|\omega_r/\omega_0$.

$$Z_r(\omega) = \left|\frac{Z}{n}\right|\,\frac{\omega_r}{\omega_0}\,\frac{(\omega/\omega_r)^2}{1 - (\omega/\omega_r)^2 + (\omega/\omega_r)^4}\,. \quad (20)$$

The total power dissipated by the beam as a whole in the impedance is

$$P = \int \frac{d\langle I^2\rangle}{d\omega}\,Z_r(\omega)\,d\omega\,, \quad (21)$$

and the energy loss per particle in one revolution is

$$U_{pm} = \frac{eP}{I_0} = \frac{2eI_0\Gamma}{h}\left|\frac{Z}{n}\right|\frac{\omega^2}{\omega_0^2}\int_0^\infty e^{-\omega_r^2\sigma_t^2}\,\frac{\omega^2}{\omega_r^2}\,\frac{(\omega/\omega_r)^2}{1 - (\omega/\omega_r)^2 + (\omega/\omega_r)^4}\,d(\omega/\omega_r)\,. \quad (22)$$

We call the normalized convolution integral in the above equation F and substitute $y = \omega_r\sigma_t$, $x = \omega/\omega_r$,

$$F(y) = \int_0^\infty \frac{\exp(-y^2x^2)x^2\,dx}{1 - x^2 + x^4}\,. \quad (23)$$

With this we get for the directly measured and normalized loss factors k_{pm} and K_{pm}

$$k_{pm} = \frac{U_{\rm pm}}{eT_0I_0} = \frac{\Gamma}{h}\,\frac{2}{T_0}\left|\frac{Z}{n}\right|\left(\frac{\omega_r}{\omega_0}\right)^2 F(y)\,,$$
$$K_{pm} = \frac{2}{T_0}\left|\frac{Z}{n}\right|\left(\frac{\omega_r}{\omega_0}\right)^2 F(y)\,. \quad (24)$$

The dependence of the energy loss on bunch length can be approximated by a power law

$$K_{pm} = K_{pm0}\left(\frac{\sigma_0}{\sigma}\right)^a. \quad (25)$$

The exponent a can be expressed by the normalized derivative

$$a = -\frac{dK_{pm}/K_{pm}}{d\sigma/\sigma} \quad (26)$$

and for our impedance model

$$a = -\frac{dF(y)/F(y)}{dy/y}\,. \quad (27)$$

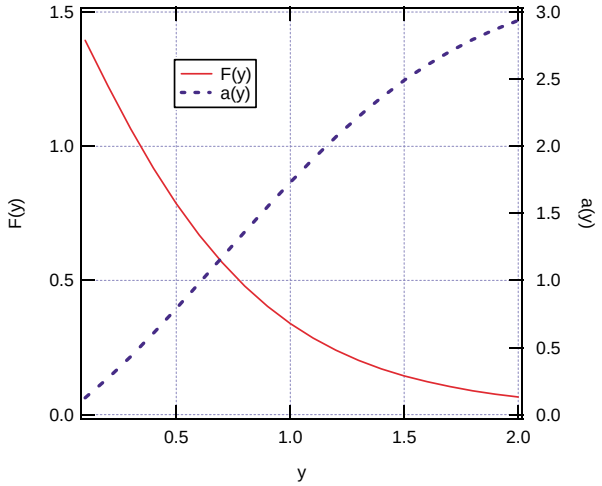

FIG. 1. (Color) Normalized convolution $F(y)$ between bunch spectrum and beam power spectrum vs bunch length times resonant frequency and the exponent a of the power law fit for the loss dependence on bunch length $U_{pm} \propto (\sigma/\sigma_0)^a$.

In Fig. 1 the normalized convolution integral $F(y)$ and the exponent a are plotted as a function of $y = \omega_r \sigma_t$. Given a bunch length σ_t and a measured bunch length dependence parameter a, these plots allow us to determine the resonant frequency of the impedance model. The shunt impedance R_s or, equivalently, the broad band impedance $|\frac{Z}{n}|$ can then be determined from the loss parameter in Eq. (24).

III. SYNCHRONOUS PHASE MEASUREMENT TECHNIQUE

Figure 2 shows the experimental setup for the phase measurements. The signals from a beam pickup and from an antenna located inside the rf cavity are filtered and observed on an HP8756A 20 GHz bandwidth digital sampling oscilloscope. The time-domain data from the scope is downloaded to a computer and Fourier analyzed, and the phases of the rf harmonic of both signals are used to obtain the relative beam-to-cavity phase. As a by-product, we also get the signal amplitude for both signals. The whole procedure is automatic and all phases and amplitudes are continuously recorded along with several machine and beam parameters.

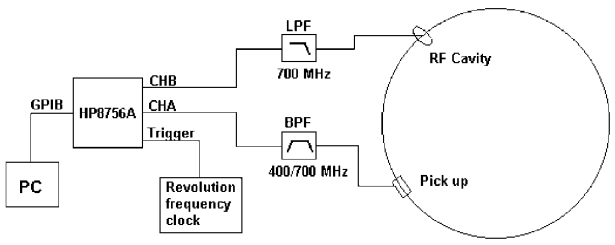

FIG. 2. Experimental setup for the synchronous phase measurement.

The oscilloscope acquisition parameters, as well as the choice of the analog filters used to condition the beam and cavity signals prior to detection, are dictated by the harmonic content of each signal and the need to eliminate unwanted harmonics. The cavity signal contains (apart from the desired rf harmonic) only components at much higher frequencies, the first higher order mode being around 720 MHz. Therefore, a 700 MHz low-pass filter is used. For the beam signal, however, contamination lines show up at multiples of the revolution frequency, so that the lines to be filtered out are much closer to the line of interest. To eliminate harmonics far away from the rf frequency, we use an analog bandpass filter made up of a combination of a 400 MHz high-pass filter and a 700 MHz low-pass filter. This is a fairly broad band device and does not suffer from the temperature stability problems of a high Q narrow band filter. In order to eliminate the remaining lines adjacent to the rf harmonic by digital filtering through the FFT analysis, the total time span for the oscilloscope acquisition must be chosen so as to provide the necessary frequency resolution according to the Nyquist criterion. On the other hand, the time resolution of the oscilloscope measurement (given by the total time span and total number of acquisition points) determines the largest frequency that can be observed, which must be higher than the upper cutoff frequency of the analog bandpass filter in order to prevent aliasing of these higher frequency components into the lower frequency spectrum. The scope acquired 1024 points in a full revolution period (310.9 ns) resulting in a time resolution of 304 ps. This corresponds to a frequency resolution of 3.2 MHz and an upper frequency cutoff of 1.64 GHz.

In order to check the data analysis routines and study the effects of random as well as systematic errors, we have used a test setup (identical with the setup used in the storage ring measurements) in which the beam and cavity signals are simulated by a synthesized rf generator. Signal averaging of many acquisitions is used to reduce the noise level, and the chosen number of acquisitions is the result of a compromise between the total acquisition time and the desired resolution. Figure 3 shows the phase noise level (as well as the total acquisition time) measured in the test bench as a function of the number of acquisitions used in signal averaging. In all later measurements we used 128 acquisitions averaging, which provides 6 mdeg rms noise level. Figure 4 shows the phase change as a function of input signal amplitude measured in the test bench. The phase remains constant to within ± 10 mdeg over a 10 dB amplitude range. Two sets of results are shown in this figure. The first set (circles) corresponds to the test setup identical with the setup used in later measurements. For the second set (squares), the bandpass filter for the beam signal is replaced with a 700 MHz low-pass filter. Both setups give equivalent results, since in the test bench the simulated beam signal has no significant harmonic component below the rf frequency.

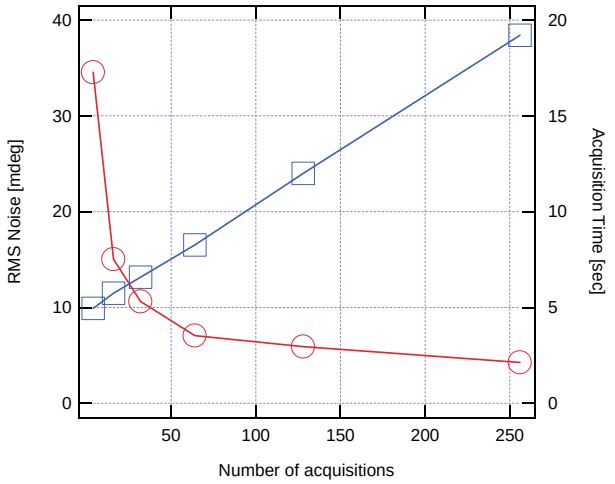

FIG. 3. (Color) Noise (rms deviation) of the relative phase measurement obtained in the test bench as a function of the number of acquisitions used in averaging. Also shown is the total acquisition time.

A nonlinear fit to a sine function was also used as an alternative data analysis procedure to cross-check the FFT results. For a pure sine wave, both fitting and FFT results for the phase variations agree to within less than 1 mdeg.

Cables from the cavity and beam pickups to the oscilloscope are a major source of systematic errors in phase measurements: temperature variations, cable motion, and contamination from other rf sources can produce sizeable phase changes. We have used Heliax FSJ1-50A cables which provide low phase temperature coefficients (about 20 mdeg/°C for our cable length and frequency), are fairly rigid, and have a solid external conductor for shielding. Also, the total cable lengths were kept to a minimum (less than 7 m) by installing the whole measurement system inside the machine tunnel and providing remote access to the oscilloscope data during measurement sessions. The cables were firmly fixed to the floor and covered with a thermal insulation foam. The cables from the cavity and pickup follow the same path for most of their length and are also in thermal contact with each other so that any remaining temperature variations affect both signals in the same way.

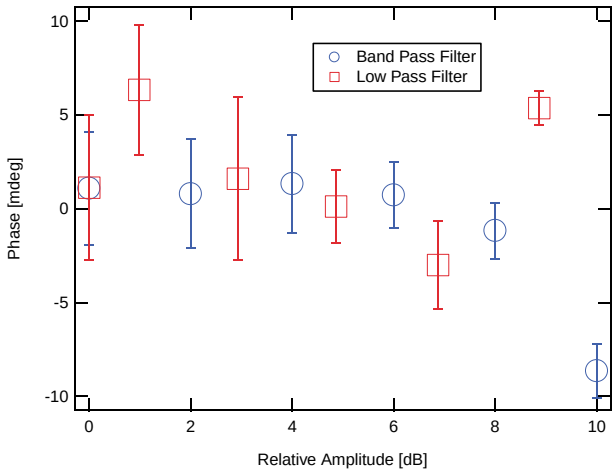

FIG. 4. (Color) Variation in the relative phase between two channels in the test setup as a function of generator output power. The circles correspond to an analog filter setup identical with the one used for later measurements with beam. The squares are results obtained with a low-pass 700 MHz analog filter for the simulated beam signal.

Measurements of the beam current and rf cavity voltage are necessary to obtain the energy loss from the phase shifts [Eqs. (5) and (8)] and therefore any systematic errors in the determination of these quantities will affect the measured losses. The beam current can be measured to very high accuracy by a commercial direct current current transformer (DCCT) whose systematic error is dominated by variations in the magnetic environment of the DCCT probe. Moreover, only variations in beam current have to be measured to determine the parasitic mode losses, and these are independent of any fixed offsets due to stray magnetic fields. Current changes as small as 10 μA can be detected. The systematic error in the determination of the gap voltage, on the other hand, is much higher and is related to errors in the calibration of the coupling of the measuring antenna in the rf cavity and the corresponding detector diode. A typical value for the uncertainty in our power measurement calibration is ± 0.5 dB, which implies $\pm 6\%$ error in the determination of the gap voltage. As a result, the same relative systematic error is expected for the measurements of the energy loss, since the gap voltage measurement sets the absolute scale for both the synchrotron radiation and parasitic mode losses.

The experiments were done in a multibunch mode with a variable gap in the bunch train, and, in order to compare the experimental results with theoretical predictions for the parasitic mode losses, we have also measured the bunch filling form factor Γ with a spectrum analyzer by measuring the squared amplitude of the revolution frequency harmonics from a beam pickup and taking the ratio of the squared amplitude of the rf harmonic to the sum of the squared amplitudes of all other harmonics in a frequency span from $f_{\mathrm{rf}}/2$ up to $3f_{\mathrm{rf}}/2$ [Eq. (18)]. Typically, the measured form factors varied from 1.0 (uniform filling) to 4.0 (partial filling) and the measurement reproducibility is of the order of 10%. The systematic error in determining the filling form factor is dominated by the uncertainty in the frequency response of the longitudinal beam pickup since we have assumed a flat frequency response of the (6 cm long) strip lines over the frequency range of interest. An estimate of the corresponding error based on the theoretical transfer impedance of the strip line gives about 3%.

IV. EXPERIMENTAL RESULTS AND DISCUSSION

Table I shows the main parameters of the LNLS electron storage ring. We performed experiments to study the

TABLE I. Main LNLS storage ring parameters.

Nominal energy	1.37	GeV
Circumference	93.2	m
Revolution frequency	3.2	MHz
rf frequency	476	MHz
Harmonic number	148	
Momentum compaction	0.0083	
Synchronous phase (at 305 kV rf voltage)	21.9	deg

synchronous phase shift as a function of rf cavity gap voltage, beam energy, and beam current.

A. Determination of the synchrotron radiation loss as a function of energy

The energy loss to synchrotron radiation is obtained from the measurement (at low beam current) of the relative phase between the beam and the cavity signal as a function of rf voltage [Eq. (5)]. Measurements have been carried out at the nominal ring energy (1.37 GeV) and at 1.15 GeV for currents below 10 mA. For such currents, the value of the parasitic mode loss, assuming an expected loss factor of the order of $K_{pm} = 10$ V/pC, in a uniform fill pattern (see next section) is of the order of 200 eV. This is only 0.2% of the calculated synchrotron radiation loss per turn, which justifies the assumption of small parasitic losses made in Eq. (3).

Figure 5 shows the result of a voltage scan at 1.15 GeV and the corresponding straight line fit. The experimental results for the energy loss at the two different energies are shown in Table II along with the theoretical predictions including the effects of fringe fields and magnet saturation (cf. the Appendix). The estimated errors in this table are obtained from the straight line fits and do not contain any contribution from systematic errors such as cavity voltage

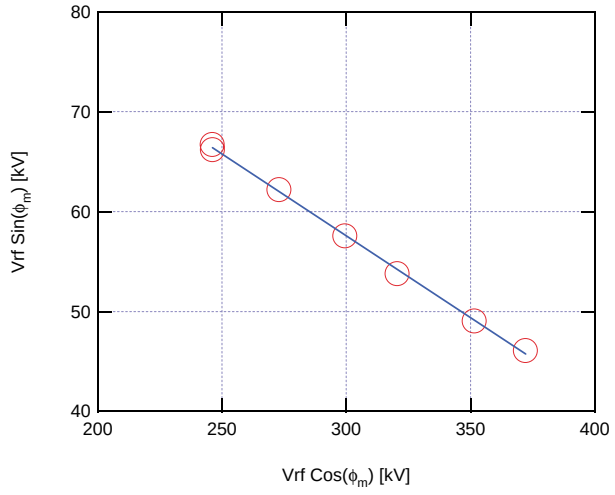

FIG. 5. (Color) Synchronous phase shift as a function of rf voltage at 1.15 GeV. Beam current is 8.3 mA.

TABLE II. Measured and calculated energy loss to synchrotron radiation at two different beam energies.

Energy (GeV)	U_s (keV) (Measured)	U_s (keV) (Calculated)
1.15	53.5 ± 1	53.6
1.37	105 ± 1	105.8

calibration. The agreement between theory and experiment is quite good.

B. Parasitic mode losses and the model impedance

The parasitic energy loss is obtained from a measurement of the relative beam-to-cavity phase as a function of beam current for a fixed cavity voltage [Eq. (8)]. The current scan is done by bringing a beam scraper close to the beam so as to reduce the beam lifetime to approximately 15 min, and the scan time is chosen as a result of a compromise between two conflicting requirements: it should be as short as possible to avoid slow temperature drifts and long enough to allow proper averaging to be done. Figure 6 shows an example of a current scan at 1.1 GeV and 305 kV gap voltage for a nearly uniform filling pattern (filling form factor = 1.0). The total change in synchronous phase during the experiment is less than 0.5 deg, and the systematic error associated with the linear approximation (small phase change) assumed in deriving Eq. (8) is about 0.2%. The fitted slope (0.055 deg/mA) corresponds to $K_{pm} = 12$ V/pC. Many such current scans were done in different machine runs, and the normalized loss factors are reproducible to within ±15%.

The use of a scraper to reduce the beam lifetime during the current scans might produce a disturbance to the impedance measurement, since the scraper itself represents

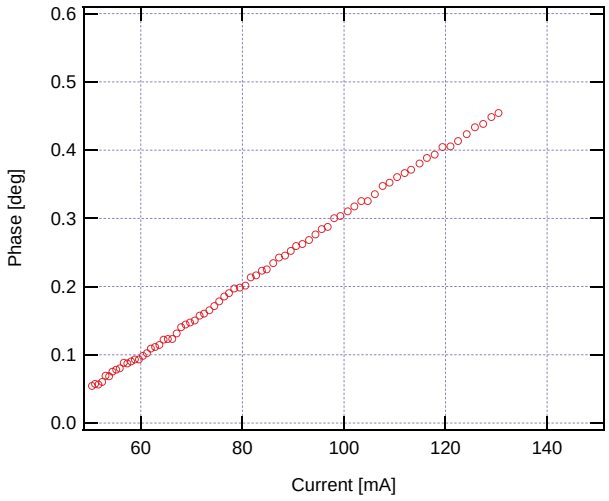

FIG. 6. (Color) Synchronous phase shift as a function of beam current at 1.1 GeV and 305 kV rf cavity gap voltage for a uniform filling. The slope gives the parasitic loss factor $K_{pm} = 12$ V/pC.

a source of impedance. We have not estimated this contribution but have done all experiments in a consistent way keeping the scraper at a fixed position during the scans. Therefore, the impedance we measured includes a possible contribution from the scraper blade. However, while bringing the scraper in at a fixed current, we did not see any measurable phase change, which indicates that this effect is small.

In order to obtain the loss parameter scaling with bunch length, the parasitic loss must be measured for various gap voltages [Eq. (25)] and various current scans must be carried out. To reduce the experiment time and avoid refills, both voltage and current scans are done in the same run by changing the current and then scanning the voltage at a (nearly) fixed current. In these runs, the beam energy was 1.1 GeV and about one-third of the ring was filled (filling form factor = 4.2). The partial fill was used in order to enhance the observed energy loss and thus make its determination easier.

Normalized loss factors obtained from two such runs are shown in Fig. 7 along with the resulting fitted values of the bunch length scaling parameter a. Taking the average of both runs, we obtain for the parameters of the broad band model

$$\frac{\omega_r}{2\pi} = 4\ \mathrm{GHz}\,, \tag{28}$$

$$\left|\frac{Z}{n}\right| = 2\Omega\,. \tag{29}$$

The value of Z_n is in good agreement with estimates of the chamber impedance made during machine design [7], and the resonant frequency is about a factor of 2 larger than expected from a rough calculation based on the vacuum chamber radius (30 mm).

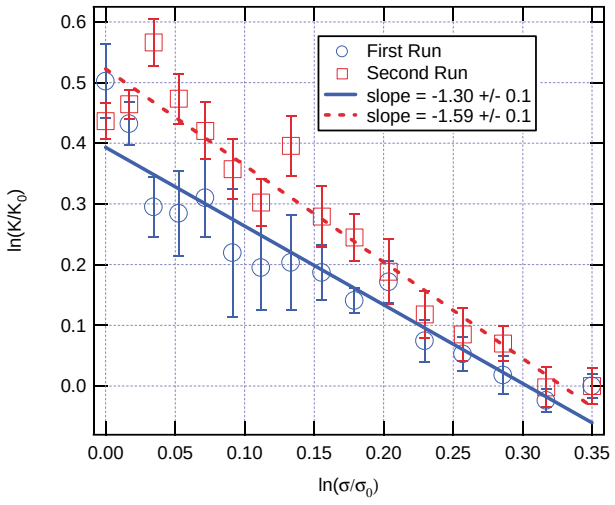

FIG. 7. (Color) Normalized parasitic mode losses determined from current scans at different rf cavity voltages in two different runs. The slopes give the impedance model parameter a. We have used rf voltages ranging from 216 to 426 kV.

C. Conclusions

We have described the use of a digital sampling oscilloscope to measure accurately the synchronous phase shift in an electron storage ring. The phase measurement system has resolution better than 6 mdeg, and the sensitivity to input signal amplitude variations is less than ± 10 mdeg over 10 dB input signal amplitude range. The variation of phase as a function of beam current and rf cavity voltage was used to determine the loss to synchrotron radiation and the parasitic losses to the resistive impedance. The resulting synchrotron radiation losses have the expected energy scaling when magnet saturation is taken into account and the dependence of the losses on bunch length are consistent with a broad band model with a resonant frequency of 4 GHz and a broad band impedance $|\frac{Z}{n}| = 2\Omega$.

APPENDIX: THE CALCULATED ENERGY LOSS DUE TO SYNCHROTRON RADIATION

The energy loss per turn to synchrotron radiation is obtained by integrating the radiated power over one revolution [1]

$$U_s = \oint P\,dt = \frac{2r_0c^2e^2E^2}{3(m_0c^2)^3}\oint B^2\,ds = \frac{2r_0E^4}{3(m_0c^2)^3}\oint\frac{ds}{\rho^2}\,, \tag{A1}$$

with $1/\rho$ being the local radius of curvature. The synchrotron radiation integral can be expressed by an effective quadratic length defined by an integral over a single magnet

$$\ell_2 = \rho_0^2\int\frac{ds}{\rho^2}\,, \tag{A2}$$

where ρ_0 is the radius of curvature at the magnet center, and we get for the energy loss per turn

$$U_s = \frac{2r_0E^4}{3(m_0c^2)^3}\,\frac{12}{\rho_0^2}\,\ell_2\,. \tag{A3}$$

The effective quadratic length is obtained from magnetic measurements, and, due to saturation effects, it depends on the magnet current. For the case of the LNLS magnets that effect accounts for about 10% reduction of the energy loss at full current.

[1] H. Wiedemann, *Particle Accelerator Physics* (Springer-Verlag, Berlin, 1993).
[2] L. Rivkin, J. P. Delahaye, K. Wille, M. Allen, K. Bane, T. Fieguth, A. Hofmann, A. Hutton, M. Lee, W. Linebarger, P. Morton, M. Ross, R. Ruth, H. Schwarz, J. Seeman, J. Shepard, R. Stiening, P. Wilson, and M. Woodley, IEEE Trans. Nucl. Sci. **32**, 2626 (1985).
[3] M. A. Allen, J. M. Paterson, J. R. Rees, and P. B. Wilson, IEEE Trans. Nucl. Sci. **22**, 1838 (1975).

[4] W. Anders, P. Kuske, and T. Westphal, in *Proceedings of the European Particle Accelerator Conference, Berlin, 1992* (Editions Frontíeres, Gif-sur-Yvette, France, 1992), p. 1121.

[5] K. Nakajima, M. Ohno, A. Ogata, and E. Ezura, in *Proceedings of the Fifth Symposium on Accelerator Science and Technology in Japan, Tsukuba, Japan, 1984* (KEK, Tsukuba, 1984), p. 300.

[6] B. Podobedov and R. Siemann, Phys. Rev. ST Accel. Beams **1**, 072801 (1998).

[7] L. Lin, L. Jahnel, and P. F. Tavares, LNLS Report No. MeT 09/91, 1991.